Journal of Radiation Research, Vol. 59, No. 2, 2018, pp. 129–140
doi: 10.1093/jrr/rrx101
Advance Access Publication: 27 January 2018

Induction of autophagy and interleukin 6 secretion in bystander cells: metabolic cooperation for radiation-induced rescue effect?

Eva Yi Kong[1], Shuk Han Cheng[2,3] and Kwan Ngok Yu[1,3,*]

[1]Department of Physics, City University of Hong Kong, Tat Chee Avenue, Kowloon Tong, Hong Kong
[2]Department of Biomedical Sciences, City University of Hong Kong, Tat Chee Avenue, Kowloon Tong, Hong Kong
[3]State Key Laboratory in Marine Pollution, City University of Hong Kong, Tat Chee Avenue, Kowloon Tong, Hong Kong
*Corresponding author: Tel: +852-344-27812; Fax: +852-344-20538;
Email: peter.yu@cityu.edu.hk
(Received 6 October 2017; revised 1 December 2017; editorial decision 22 December 2017)

ABSTRACT

We hypothesized that radiation-induced rescue effect (RIRE) shared similar mechanisms with 'metabolic cooperation', in which nutrient-deprived cancer cells prompted normal cells to provide nutrients. Our data demonstrated that X-ray irradiation induced autophagy in HeLa cells, which could last at least 18 h, and proved that the irradiated cells (IRCs) resorted to breaking down their own intracellular components to supply the molecules required for cell-repair enhancement (e.g. to activate the NF-κB pathway) in the absence of support from bystander unirradiated cells (UICs). Furthermore, autophagy accumulation in IRCs was significantly reduced when they were partnered with UICs, and more so with UICs with pre-induced autophagy before partnering (through starvation using Earle's Balanced Salt Solution), which showed that the autophagy induced in UICs supported the IRCs. Our results also showed that interleukin 6 (IL-6) was secreted by bystander UICs, particularly the UICs with pre-induced autophagy, when they were cultured in the medium having previously conditioned irradiated HeLa cells. It was established that autophagy could activate the signal transducer and activator of transcription 3 (STAT3) that was required for the IL-6 production in the autophagy process. Taken together, the metabolic cooperation of RIRE was likely initiated by the bystander factors released from IRCs, which induced autophagy and activated STAT3 to produce IL-6 in bystander UICs, and was finally manifested in the activation of the NF-κB pathway in IRCs by the IL-6 secreted by the UICs.

Keywords: autophagy; ionizing radiation; rescue effect; bilateral bystander effect; bidirectional signaling; reciprocal bystander effect

INTRODUCTION

Radiation-induced bystander effect (RIBE) refers to the phenomenon that unirradiated cells (UICs) respond as if they have been irradiated after they have partnered with the irradiated cells (IRCs) or after they have been treated with the medium previously conditioning the IRCs. Two mechanisms underlying RIBE have been widely adopted, namely, (i) gap junction intercellular communication (when there is cell–cell contact), and (ii) communication of soluble signal molecules released by IRCs into the medium conditioning the IRCs. Radiation-induced rescue effect (RIRE) is closely related to RIBE and describes the phenomenon that IRCs derive benefits from feedback signals released from bystander UICs, e.g. the UICs can alleviate the harmful radiobiological effects in the IRCs. In 2011, RIRE was demonstrated between human primary fibroblast (NHLF) and human cervical cancer (HeLa) cells [1]. RIRE has since attracted extensive interest in the research community, and has been successfully demonstrated in different *in vitro* [2–10] and *in vivo* [11, 12] experiments. A review summarized recent studies on RIRE, as well as possible mechanisms and the involved chemical messengers [13]. In particular, it was also revealed that RIRE was induced in α-particle–irradiated HeLa and NIH/3T3 cells through activation of the nuclear factor kappa B (NF-κB) pathway in the IRCs [5].

Interestingly, RIRE bears some resemblance to the metabolic cooperation between cancer cells and normal cells (e.g. see review in Ref. [14]). In a tumor microenvironment, when the vascular supply of nutrients to the cancer cells becomes limiting, neighboring normal cells can be prompted to provide nutrients to support the survival and growth of the cancer cells [15–19]. Metabolic cooperation has also been found between cancer cells in a tumor and normal cells in distant tissues or organs [20, 21].

The objective of the present paper was to explore the similarity between metabolic cooperation and RIRE, with a view to proposing a unified scheme in which these seemingly different processes are in fact only different manifestations. The similarity would become apparent if the nutrient-depleted cancer cells and the IRCs were generalized as 'stressed cells', while the normal cells metabolically cooperating with the nutrient-depleted cancer cells and the UICs partnering with the IRCs were generalized as 'bystander cells'. Such a unified scheme could help us gain new insights into the different processes, which might help improve the efficacy of the related therapy methods.

The finding that RIRE was triggered through NF-κB activation in the IRCs [5] pointed to a potential involvement of autophagy in the process, since NF-κB repressed autophagy [22], while autophagy regulated the NF-κB pathway [23], and there was complex interplay between the two pathways [24, 25]. Autophagy plays a fundamental role in cellular homeostasis by inducing recycling of damaged organelles and toxic components [26–29]. There are excellent reviews on the role played by autophagy in both physiological and pathological cell death [30, 31]. Autophagy can be activated by adverse stimuli, including oxidative stress, DNA damage, and starvation for nutrients such as amino acids [32–35]. In particular, under starvation, it can lead to breakdown of intracellular components within lysosomes to supply energy to enhance cell survival [31, 36]. If autophagy is induced in IRCs by ionizing radiation, it is also natural that autophagy is induced in UICs following the general pattern for RIBE in that 'unirradiated cells responded as if they had been irradiated'. As such, in the present paper, we chose for our reference a metabolic cooperation process involving autophagy in the involved cells. We compared our IRC/UIC system (with IRCs and UICs) to the PCC/PSC system where autophagy was promoted in non-cancerous pancreatic stellate cells (PSCs) to release alanine to help neighboring pancreatic cancer cells (PCCs) survive in the tumor microenvironment [18]. According to our unified scheme described above, the PCCs were the 'stressed cells', while the PSCs were the 'bystander cells'. Table 1 compares the PCC/PSC system and the IRC/UIC system, and we hypothesize that the processes in the two systems share similar mechanisms.

Inspired by the PCC/PSC system, we aimed to prove that autophagy pre-induction in bystander UICs (before partnering with IRCs) would enhance RIRE in IRCs. While autophagy has previously been shown to be induced in UICs upon partnering with IRCs irradiated by heavy ions [37] and γ-rays [38], support provided to IRCs as a result of autophagy in UICs has not been demonstrated. Furthermore, if autophagy in UICs provides support to IRCs, it would also be likely that IRCs would resort to breaking down their own intracellular components to supply molecules required in the absence of UICs.

In a previous study [5], activation of the NF-κB pathway was shown [through the use of the NF-κB activation inhibitor BAY-11–7082 (IκB phosphorylation inhibitor) as well as through staining for phosphorylated NF-κB (p-NF-κB) expression using the anti-NF-κB p65 (phospho S536) antibody] to be involved in RIRE in HeLa cells irradiated by α particles. In order to provide further mechanistic insight, extra experiments were performed in order to study the secretion of interleukin 6 (IL-6) by bystander cells when cultured in medium that had previously conditioned irradiated HeLa cells. As accumulating evidence showed that the inflammatory cytokine IL-6 could activate the NF-κB pathway [39–42], it would be pertinent to explore whether IL-6 was involved in RIRE in the studied IRC/UIC system.

Accordingly, the objectives of the present paper were to study (i) whether autophagy is induced in IRCs by ionizing radiation and also in bystander UICs, (ii) whether IL-6 secretion is induced in bystander UICs, and (iii) whether autophagy pre-induction in bystander UICs enhances IL-6 secretion in these UICs as well as RIRE in IRCs.

MATERIALS AND METHODS

Materials and chemicals

Dulbecco's Modified Eagle Medium (DMEM) (Gibco, USA), fetal bovine serum (FBS) (Gibco, USA), LysoTracker Red DND-99 (LysoTracker, USA), secondary Alexa Fluor488 goat anti-rabbit IgG

Table 1. Comparisons between PCC/PSC system and IRC/UIC system

	PCC/PSC system	IRC/UIC system
Stressed cells	Pancreatic cancer cell (PCC) (in low-nutrient environment)	Irradiated cell (IRC)
Bystander cells	Pancreatic stellate cell (PSC)	Unirradiated cell (UIC)
Benefits to stressed cells	Proliferation while deprived of nutrients	Activate NF-κB pathway (while deprived of signal molecules?) to enhance cell survival
Bystander factors	Unknown	Multiple: including TNF-α, TGF-β1, IL-6, IL-8, NO and ROS
Manifestations in bystander cells	Induces autophagy [26]	Induces autophagy [45, 46]
Rescue factors	Amino acid (Ala) [26]	IL-6

antibody (Invitrogen, USA), human IL-6 ELISA (NOVEX, USA), Earle's balanced salt solution (Gibco, USA), phosphate buffered saline (PBS) (Gibco, USA) and 16% formaldehyde (Pierce, USA) were purchased from Thermo Fisher Scientific Inc. The Cyto-ID Autophagy detection kit (Enzo Life Sciences, USA) was purchased from Boppard (H.K) Co. Ltd. Primary anti-53BP1 antibody (Abcam, USA) was purchased from Abcam (H.K) Ltd. Goat serum (Sigma-Aldrich, USA) and Triton-X 100 (Sigma-Aldrich, USA) were purchased from Tin Hang Technology (H.K) Ltd.

Cell culture

The HeLa cells (ATCC® CCL-2™) were obtained from American Type Culture Collection. The cells were routinely cultured in DMEM, supplemented with 10% FBS and incubated at 37°C in an atmosphere with a humidified 5% CO_2 incubator. Previous evidence showed that HeLa cells subjected to Earle's Balanced Salt Solution (EBSS) for starvation could lead to autophagy [43, 44]. To prepare starved HeLa cells, a total of 2×10^5 HeLa cells were seeded in each 35 mm petri dish overnight, and the cells were then treated with EBSS for 4 h.

X-ray irradiation

X-ray irradiation was performed using the X-ray generator, X-RAD 320 irradiator (Precision X-ray Inc., North Branford, CT, USA), with voltage and current set at 200 kV and 10 mA, respectively, and employing a 2 mm thick aluminum (Al) filter to harden the X-ray, while the source-to-surface distance was set as 50 cm. The dose rate was ~0.9 Gy/min. Tailor-made 35 mm petri dishes with a hole (diameter = 6.5 mm) at the center covered by a glass coverslip on the bottom were employed for the experiments. A total of 10^4 HeLa cells were plated on the glass coverslip and incubated overnight before X-ray irradiation. HeLa cells were irradiated by X-rays with a dose of 2 Gy (the IRCs) before being partnered with bystander UICs for 4 or 18 h.

Preparation of irradiated and rescued HeLa cells

A total of 5×10^4 HeLa cells were plated on 22 × 22 mm glass coverslips and incubated overnight. UICs were first divided into two groups and subjected to different treatments for 4 h, namely, (i) those treated with complete medium (i.e. DMEM with 10% FBS): referred to as the BY_{DMEM} group and (ii) those treated with EBSS: referred to as the BY_{EBSS} group (for pre-induction of starvation) for 4 h, before being partnered with IRCs for a further 4 or 18 h. The IRCs partnered with the BY_{DMEM} and BY_{EBSS} groups were referred to as RE and EBSS RE groups, respectively, while the IRCs without partnering were referred to as the 2 Gy group. Figure 1 schematically shows the procedures for preparation and partnering.

Autophagy induction in bystander cells

A total of 2×10^5 HeLa cells were seeded in each 35 mm petri dish overnight. The HeLa cells were then irradiated with X-rays with a dose of 2 Gy (IRCs). At 4 h post irradiation, the medium conditioning the irradiated cells was collected and transferred to the bystander cells (BY group). At the same time, medium conditioning the sham-irradiated cells was also collected and transferred to the bystander cells (SBY group).

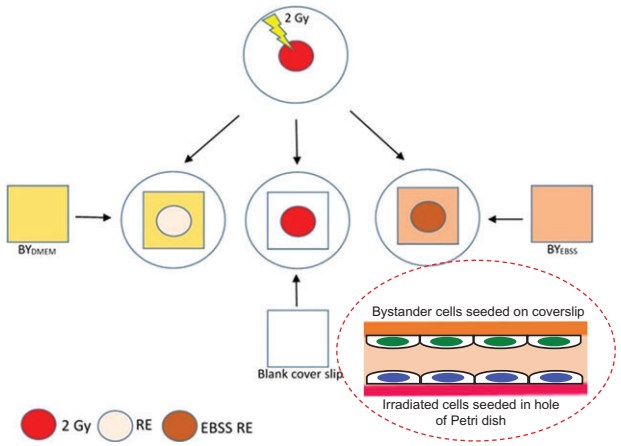

Fig. 1. Schematic diagram showing the procedures for preparation and partnering for the 2 Gy, RE and EBSS RE groups. Unirradiated cells (UICs) were first divided into two groups and subjected to different treatments for 4 h, namely, (i) those treated with complete medium (i.e. Dulbecco's Modified Eagle Medium with 10% fetal bovine serum): referred to as the BY_{DMEM} group and (ii) those treated with Earle's Balanced Salt Solution: referred to as the BY_{EBSS} group (for pre-induction of starvation) for 4 h, before being partnered with irradiated cells (IRCs) for a further 4 or 18 h. The IRCs partnered with the BY_{DMEM} and BY_{EBSS} groups are referred to as RE and EBSS RE groups, respectively, while the IRCs without partnering are referred to as the 2 Gy group.

The SBY group acted as the experimental control group. After 4 h of incubation with the transferred conditioned medium, both BY and SBY groups of HeLa cells were analyzed by LysoTracker Red staining.

53BP1 immunofluorescent staining

To evaluate the radiation-induced DNA damages in terms of double-strand breaks (DSBs), the expression of 53BP1 in the HeLa cells was assayed. The cells were washed with PBS before fixation in 4% formaldehyde at room temperature at 4 or 18 h post irradiation, then washed three times with PBS, permeabilized in 0.5% Triton X-100 at 37°C, and finally incubated with 1.5% goat serum blocking solution followed by primary anti-53BP1 antibody (1:500) at 37°C for 1.5 h. The cells were further washed with PBS three times, and incubated with secondary Alexa Fluor-488 goat anti-rabbit IgG antibody (1:1000) at 37°C for 1 h. Fluorescence images were captured with a Nikon Ti-E motorized inverted fluorescence microscope (Nikon Instruments Inc., Melville, NY, USA) with an objective magnification of ×40. At least 100 cells in each sample were counted. Quantification of 53BP1 foci was analyzed using the NIS-Elements Advanced Research software (Nikon Instruments Inc., Melville, NY, USA).

LysoTracker Red and Cyto-ID staining

For studying the acidic organelles in the HeLa cells, 500 nM LysoTracker Red was employed. LysoTrakcer Red is a fluorescent

acidotropic probe widely used to reveal autophagic activity by labeling and tracking acidic vesicular organelles (AVOs) in live cells such as endosomes, lysosomes and autolysosomes [45–47].

At the same time, Cyto-ID (after dilution according to the manufacturer's recommended staining procedures) was used to reveal the autophagic flux. The Cyto-ID assay was previously shown to be more sensitive and reliable than the specific monodansylcadaverine (MDC) spectrophotometric *in vivo* assay for autophagic vacuoles, as well as the well-established LC3B immunoblotting assay widely used in monitoring autophagy [48].

In the present work, the cells were counterstained with LysoTracker Red and Cyto-ID in serum-free culture medium [49] for 30 min at 37°C at 4 or 18 h post irradiation. After staining, the cells were washed with PBS three times and then fixed in 4% formaldehyde at room temperature. All images were captured using the fluorescence microscope with an objective magnification of ×40 under identical conditions in each experiment. At least 100 cells in each sample were counted. The fluorescence intensity was analyzed using the NIS-Elements Advanced Research software (Nikon Instruments Inc., Melville, NY, USA). The autophagy activity factor (*AAF*) was calculated using the equation:

$$AAF = [MFI\,(treated) - MFI\,(control)]/MFI\,(treated) \times 100$$

where *MFI* = mean fluorescence intensity. *AAF* is a quantitative method commonly employed to quantify autophagic flux [50, 51], which has been adopted to measure the level of autophagic accumulation within a cell population in the present study.

Determination of interleukin 6 concentrations in conditioned media using an enzyme-linked immunosorbent assay (ELISA)

A total of 2×10^5 HeLa cells were seeded in each 35 mm petri dish overnight. The control group was denoted 'the ctl group', while 'the EBSS group' was the group of HeLa cells first treated with EBSS for 4 h and then incubated with fresh DMEM with 10% FBS for a further 4 h. At 4 h post irradiation by 2 Gy X-rays, the medium having conditioned the IRCs was collected, and (i) transferred to the cultures of UICs treated with DMEM with 10% FBS for incubation for a further 4 h ('the BY group'), or (ii) transferred to the cultures of UICs treated with EBSS for incubation for a further 4 h ('the EBY group') or (iii) incubated alone for a further 4 h (the '2 Gy group'). After 4 h incubation, the media from the different groups (ctl, EBSS, 2 Gy, BY and EBY) were collected and centrifuged at 1500 rpm for 10 min at 4°C to remove the cells or cellular debris. The IL-6 concentrations (pg/ml) in the media were measured using an IL-6 ELISA kit following the manufacturer's instructions. The results were obtained from three independent experiments.

Statistical analysis

Statistical analyses were performed on the means of the data obtained from at least three independent experiments and performed in triplicates. All the results were presented as means ± SEMs. Differences between two groups of data were analyzed using Student's *t*-test. On the other hand, differences between more than two groups of data were analyzed using one-way analysis of variance (ANOVA), and if statistically significant ($P < 0.05$) the differences between two particular groups of data were analyzed using Least Significant Difference (LSD) *post-hoc t*-tests. A *P* value of <0.05 was considered as indicating a significant difference between the compared groups.

RESULTS

Rescue effect in HeLa cells exposed to X-ray irradiation

Figure 2 shows the results for 53BP1 expression in different groups at 4 and 18 h post irradiation. At the early stage (4 h post irradiation), there were no significant differences in the numbers of 53BP1 foci/cell

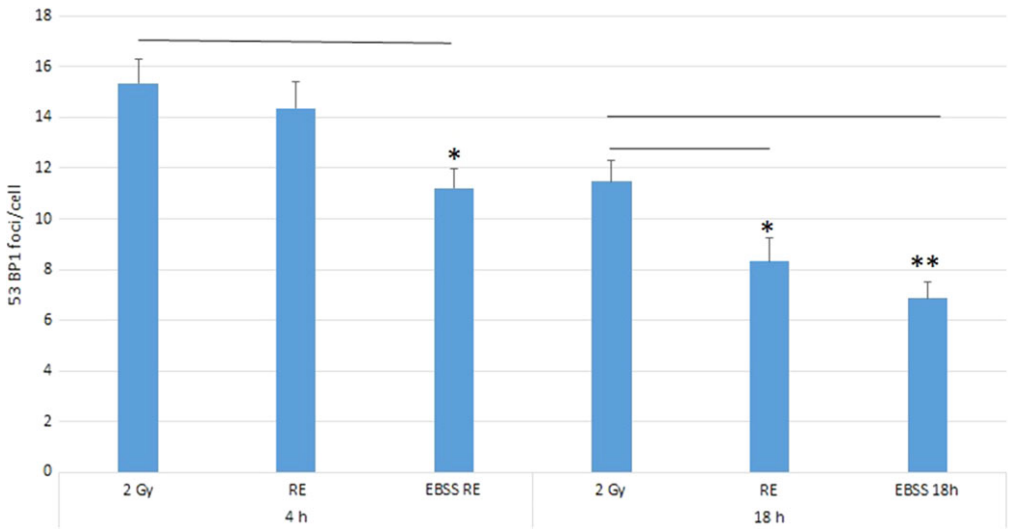

Fig. 2. Number of 53BP1 foci/cell nucleus in 2 Gy, RE and EBSS RE groups of HeLa cells at 4 and 18 h post irradiation. Independent experiments were performed in triplicate and repeated three times. Data were analyzed using one-way ANOVA followed by *post-hoc t*-tests. *$P < 0.05$, **$P < 0.01$ and error bars represent ± SEM.

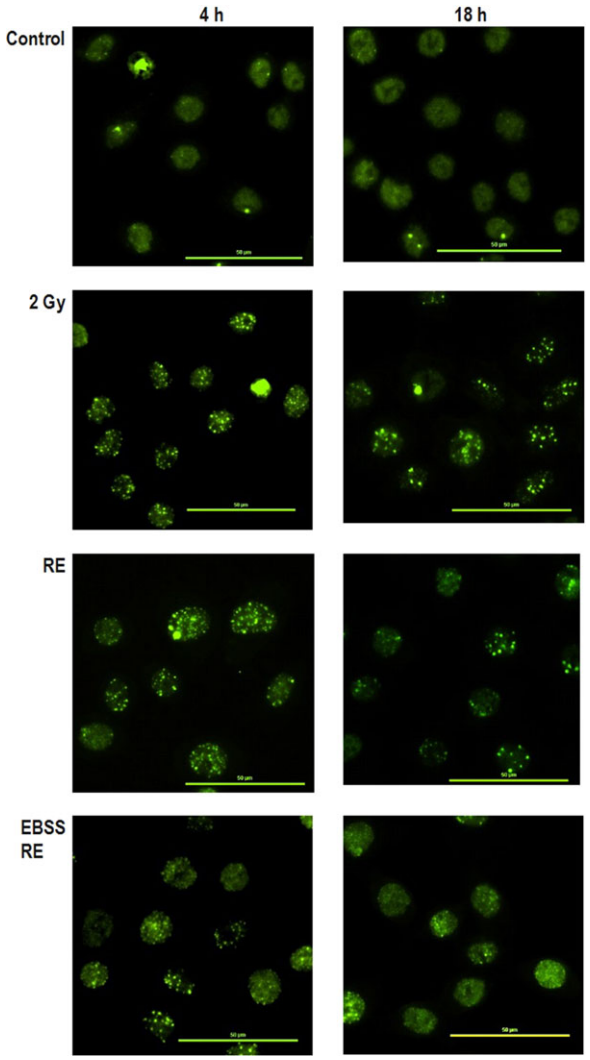

Fig. 3. Representative immunofluorescence 53BP1 staining results captured using a fluorescence microscopy at ×40 magnification of HeLa cells after 4 and 18 h irradiation. Scale bar = 50 μm.

nucleus between the irradiated group (2 Gy group) (15.3 ± 1.0) and the rescued group (RE group; IRCs co-cultured with UICs treated with DMEM (BY_{DMEM})) (14.4 ± 1.3). Interestingly, however, the EBSS RE group [IRCs co-cultured with UICs treated with EBSS (BY_{EBSS})] showed a decrease in 53BP1 accumulation (11.2 ± 0.9), indicating the presence of a rescue effect at the early stage. At the late stage (18 h post irradiation), the numbers of 53BP1 foci/nucleus in all groups dropped when compared with their counterparts at the early stage. At 18 h post irradiation, there were significant decreases in the numbers of 53BP1 foci/nucleus in both the RE group (8.3 ± 0.9) and the EBSS RE group (6.9 ± 0.7) compared with the 2 Gy group (11.5 ± 0.8), and the number of 53BP1 foci/nucleus in the EBSS RE group was smaller than that in the RE group. Figure 3 shows representative immunofluorescence 53BP1 staining results of HeLa cells after 4 and 18 h irradiation.

Pre-induction of autophagy by EBSS starvation in HeLa cells

As described above, HeLa cells were starved using EBSS to pre-induce autophagy before their partnering with the IRCs. Figure 4a shows representative LysoTracker Red staining results of control HeLa cells and those subjected to EBSS starvation for 4 h. Figure 4b shows the fold changes in LysoTracker Red fluorescence intensities in ctl and EBSS 4h (HeLa cells treated with EBSS for 4 h) groups of HeLa cells (normalized to that for the control 'ctl'). The results show that the LysoTracker Red fluorescence intensity in starved HeLa cells [(1.63 ± 0.07)-fold increase relative to the control] was significantly higher than the fluorescence intensity for the control group.

Autophagy induction in bystander cells

Figure 5a shows the fold changes in LysoTracker Red fluorescence intensities (normalized to that for the experimental control) of bystander HeLa cells (BY group: bystander cells partnered with irradiated cells; and SBY group: bystander cells partnered with sham irradiated cells) cultured for 4 h in the medium having previously conditioned HeLa cells irradiated with 2 Gy X-ray. The fold change for the BY group was larger with statistical significance ($P < 0.05$) than that for the SBY group, which showed that autophagy was activated in the bystander cells. On the other hand, Fig. 5b shows the average number of 53BP1 foci/cell nucleus in the BY DMEM group (normal bystander cells treated with DMEM) and the BY EBSS group (EBSS treated bystander cells) of HeLa cells recorded at 4 h post irradiation. The average number of 53BP1 foci/cell nucleus in the BY DMEM group was significantly larger than that for the BY EBSS group ($P < 0.01$), which showed that pre-induction of autophagy in the bystander cells could mitigate the damages brought by RIBE.

Autophagy induction in HeLa cells upon 2 Gy X-ray irradiation

Figure 6 shows the fold changes in the LysoTracker Red fluorescence intensities in HeLa cells at 4 and 18 h post irradiation. At 4 h post irradiation, LysoTracker Red was accumulated in HeLa cells irradiated with 2-Gy X-rays [(4.75 ± 0.18)-fold increase cf. control]. In relation, there was a significantly lower level of LysoTracker Red intensity in the EBSS RE group [(1.61 ± 0.03)-fold increase cf. control]. Although the LysoTracker Red intensity dropped in the RE group [(2.96 ± 1.03)-fold increase cf. control], the difference was not significant compared with the IR group. At 18 h post irradiation, the results showed that acidic vesicular organelles (AVOs) were still accumulated in HeLa cells irradiated with 2-Gy X-rays, and the LysoTracker Red intensity was the highest [(5.40 ± 0.90)-fold increase cf. control] among all groups. However, the LysoTracker Red intensity dropped significantly in both the RE group and the EBSS RE group [(1.30 ± 0.21)-fold and (1.18 ± 0.23)-fold increase cf. control, respectively].

We further confirmed autophagy accumulation in irradiated HeLa cells using the Cyto-ID Autophagy Detection assay. Table 2 shows the mean values of autophagy activity factor (*AAF*) for different groups. The results demonstrated that at the early stage (4 h post irradiation), the percentage of cells expressing active

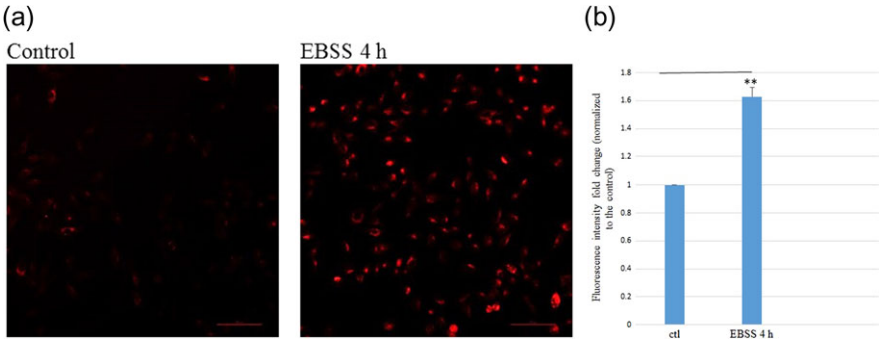

Fig. 4. Data of starvation of HeLa cells by EBSS. (a) Representative LysoTracker Red staining results of control HeLa cells and those subjected to EBSS starvation for 4 h captured using a fluorescence microscope at ×20 magnification. Scale bar = 100 µm. (b) Fold changes in LysoTracker Red fluorescence intensities in ctl and EBSS 4h (HeLa cells treated with EBSS for 4 h) groups of HeLa cells (normalized to that for the control 'ctl'). Independent experiments were performed in triplicates and repeated three times. $^{**}P < 0.01$, and error bars represent ± SEM.

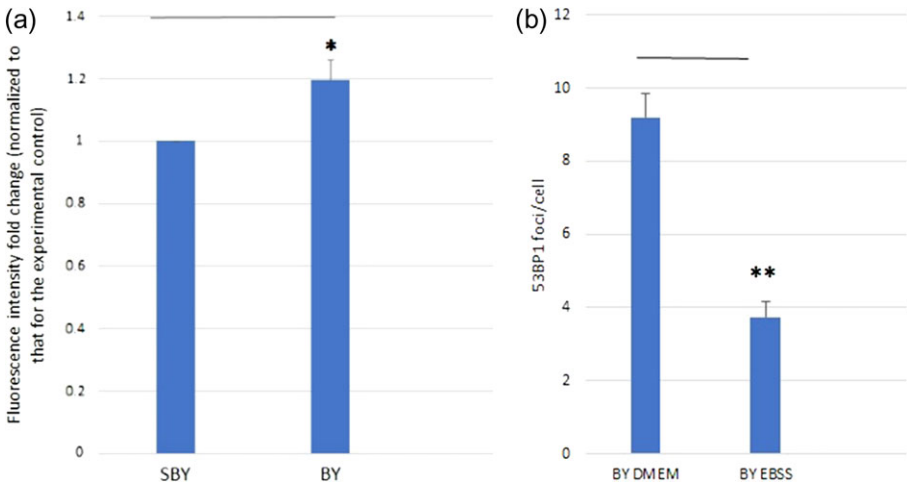

Fig. 5. Results for bystander cells. (a) Fold changes in LysoTracker Red fluorescence intensities (normalized to that for the experimental control) of bystander HeLa cells (BY group and SBY group) cultured for 4 h in the medium having previously conditioned HeLa cells irradiated with 2 Gy X-ray. ($n = 3$) (b) Number of 53BP1 foci/cell nucleus in BY DMEM group and BY EBSS group of HeLa cells recorded at 4 h post irradiation. Independent experiments were performed in triplicates and repeated three times. $^{*}P < 0.05$, $^{**}P < 0.01$, and error bars represent ± SEM.

autophagic vacuoles was significantly decreased in the EBSS RE group (29.4 ± 9.0%) compared with the 2 Gy group (68.0 ± 2.2%). The percentage of autophagic vacuoles in the RE group (48.4 ± 9.2%) dropped, although not significantly compared with the IR group. At a later stage (18 h post irradiation), the percentage of cells expressing active autophagic vacuoles was significantly decreased in both RE (39.8 ± 2.7%) and EBSS RE (18.8 ± 3.4%) groups. In contrast, accumulation of autophagic vacuoles was still maintained at a high level in the 2 Gy group (72.9 ± 2.4%). Figures 7 and 8 show representative microscopic fields of HeLa cells with active autophagy (green) and AVOs (red) counterstained with Hoechst 33342 in different groups at 4 and 18 h post irradiation, respectively.

IL-6 induction in bystander HeLa cells

Figure 9 shows the IL-6 concentrations (pg/ml) measured using ELISA in conditioned media from HeLa cells in different groups, namely, the control group (ctl), the group treated with EBSS for 4 h and then incubated with fresh DMEM with 10% FBS for 4 h (EBSS group), 2 Gy, BY and EBY groups. Interestingly, the IL-6 concentrations in the conditioned media were in the order EBY > BY > 2 Gy groups, and the difference between the EBY and the 2 Gy groups was statistically significant ($P < 0.01$). These observations supported the hypothesis that IL-6 was secreted in the bystander cells and that IL-6 was a cytokine communicated between the irradiated and bystander HeLa cells.

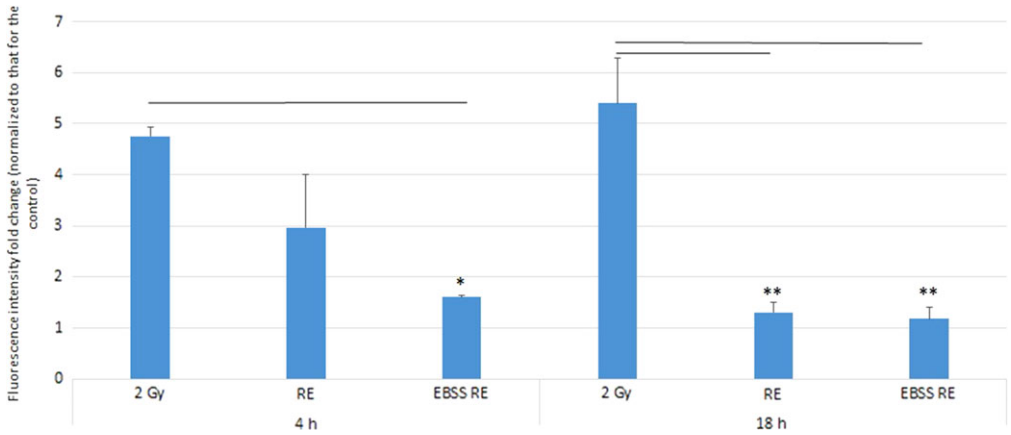

Fig. 6. Fold changes in LysoTracker Red fluorescence intensities in 2 Gy, RE and EBSS RE groups of HeLa cells (normalized to those for the control group) at 4 and 18 h post irradiation. Independent experiments were performed in triplicates and repeated three times. Data were analyzed using one-way ANOVA followed by *post-hoc t*-tests. *$P < 0.05$, **$P < 0.01$ and error bars represent ± SEM.

Table 2. Mean values of AAF (± SEM) in irradiated HeLa cells

	Autophagy Activity Factor (AAF) (%)	
	4 h	18 h
2 Gy	68.0 ± 2.2	72.9 ± 2.4
RE	48.4 ± 9.2	39.8 ± 2.7**
EBSS RE	29.4 ± 9.0*	18.8 ± 3.4**

Independent experiments performed in triplicate and repeated three times. *$P < 0.05$ and **$P < 0.01$.

DISCUSSION

Rescue effect in HeLa cells exposed to X-ray irradiation

DNA damages in HeLa cells inflicted by an X-ray dose of 2 Gy were examined in the present study through the expression of 53BP1. Figure 2 shows that only the EBSS RE group displayed the rescue effect at the early stage (4 h post irradiation), while both the RE and EBSS RE groups displayed the rescue effect at the late stage (18 h post irradiation). The results were consistent with previous findings which showed that the ratios between the numbers of 53BP1 foci on IRCs in the presence and absence of bystander cells were relatively small for time-points of 5 h or less post-irradiation [5].

Previous studies showed that 53BP1 foci did not completely disappear after 8 h treatment, and residual 53BP1 foci could even remain at 24 h post-irradiation [1, 52, 53].

Autophagy in irradiated cells

Our data demonstrated that X-ray irradiation induced autophagy in HeLa cells, and the promotion of autophagy lasted at least 18 h after irradiation. Previous research revealed accumulation of autophagy in different cell lines upon irradiation with heavy ions with high linear-energy-transfer (LET) values [54–58]. Moreover, Hino *et al.* showed that autophagy was a fast response to heavy ion irradiation, which could be detected as soon as 30 min post irradiation [54]. By studying the human glioblastoma cell line (SHG44) and HeLa cells, Jin *et al.* showed that high-LET radiations could induce autophagy more effectively than low-LET radiations in tumor cells [58]. Our LysoTracker Red intensity data also agreed with previous findings that ionizing radiation could lead to the development of AVOs [59, 60]. Our present results further illustrated that AVOs in cells were maintained for a long period upon exposure to ionizing radiation. Autophagy induction in IRCs showed that they resorted to breaking down their own intracellular components in order to supply the required molecules in the absence of support from bystander UICs.

Autophagy in bystander cells

Figure 5a shows that autophagy was activated in the bystander cells, which is consistent with the previous finding by Hino *et al.* that autophagy was not only induced in the irradiated cells by heavy ions, but also in the bystander cells [37]. On the other hand, Fig. 5b shows that pre-induction of autophagy in the bystander cells was able to mitigate the damages brought by RIBE. Our results were commensurate with the observation of Huang *et al.* that rapamycin, one of the autophagy inducers, could inhibit RIBE in human breast cancer cells [61].

Autophagy pre-induction in bystander cells enhanced RIRE

Our data on the numbers of 53BP1 foci/cell successfully demonstrated RIRE in the RE and EBSS RE groups. At the early stage, the numbers in the EBSS RE group were significantly smaller than the corresponding numbers in the IR group. The numbers in the RE group were decreased, but without statistical significance when compared with the IR group. At the later stage, the numbers in both RE and EBSS RE groups were significantly smaller when compared

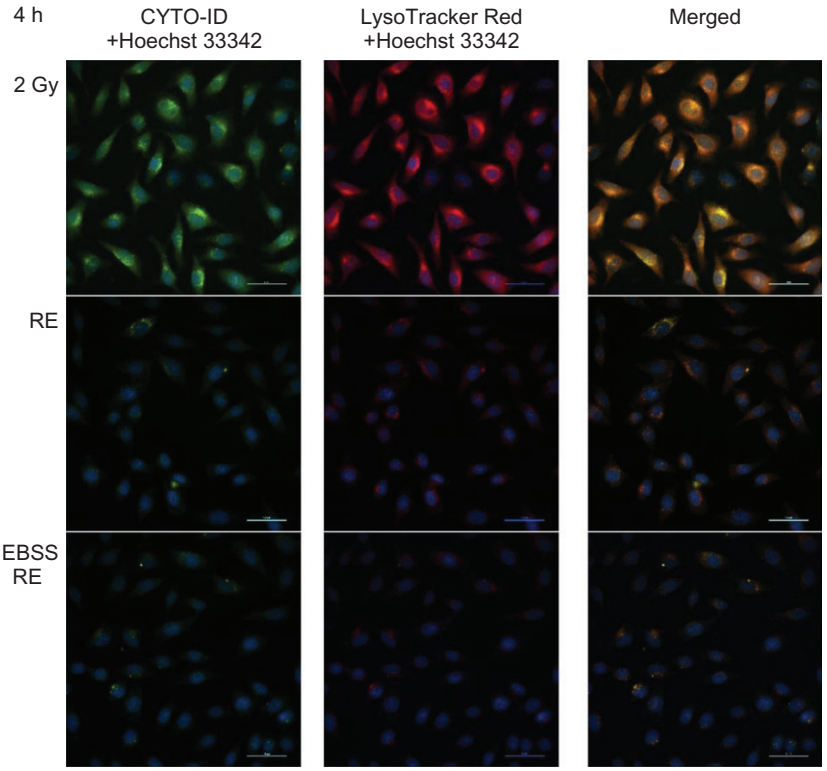

Fig. 7. Representative microscopic fields of HeLa cells with active autophagy (green) and AVOs (red) in different groups at 4 h post irradiation captured using a fluorescence microscopy at ×40 magnification. Cell nuclei were counterstained with Hoechst 33342 (blue). Scale bar = 50 μm.

with the IR group. These results on one hand illustrated that RIRE could be enhanced by promoting autophagy in bystander cells (through starvation using EBSS), and on the other hand confirmed that the significance of RIRE critically depended on the time-point, which is consistent with previous studies [1, 5]. The conclusions derived from the numbers of 53BP1 foci/cell were further supported by our LysoTracker Red intensity (AVO staining) data and Cyto-ID (autophagic vacuoles staining) data. The accumulation of AVO and autophagic vacuoles in the RE and EBSS RE groups were reduced at 4 h post irradiation, with a significant difference in the LysoTracker Red intensity and the AAF between the IR group and the EBSS RE group. Both RE and EBSS RE groups showed significant differences in the LysoTracker Red intensity and the AAF when compared with the IR group at 18 h post irradiation.

IL-6 as a rescue signal for RIRE

The results shown in Fig. 9 agree in general with the findings in Ref. [62] that IL-6 was suppressed in irradiated cells as well as in bystander cells. It is interesting to note from Fig. 9 that IL-6 secretion was induced in HeLa cells upon pre-treatment with EBSS, which is consistent with the previous study by Yoon *et al.* [41]. Our 53BP1 foci results showed that damages in irradiated cells partnered with EBSS-treated bystander cells were the smallest at both studied time-points (4 and 18 h), which strongly suggested that IL-6 was a rescue signal sent from bystander cells to irradiated cells, and that enhancing the production of IL-6 in bystander cells would further help rescue the irradiated cells. In relation, the 53BP1 foci results of Tamari *et al.* demonstrated that IL-6 led to radioresistance in tumor cells irradiated with γ-rays [63]. In summary, IL-6 could alleviate damages induced by ionizing radiations. Recent studies illustrated that amino-acid and serum deprivation provoked autophagic processes in HeLa cells [42], and that NF-κB activation in starved cancer cells would be affected by autophagic processes [41]. In particular, the studies showed that starvation-induced autophagy activated the signal transducer and activator of transcription 3 (STAT3), which was required for IL-6 production in the autophagy process [41, 42]. Taken together, the metabolic cooperation of RIRE was likely initiated by the bystander factors released from IRCs, which induced autophagy and activated STAT3 to produce IL-6 in UICs, and was finally manifested in the activation of the NF-κB pathway in IRCs by the IL-6 secreted by the UICs.

Insights into metabolic cooperation and RIRE processes

As explained in the Introduction, the objective of the present paper was to explore the similarity between the metabolic cooperation and the RIRE processes, with a view to establishing a unified scheme involving the 'stressed cells' and the 'bystander cells'. Upon proving that (i) autophagy was induced in the IRCs by ionizing radiation and in bystander UICs, (ii) IL-6 secretion was induced in bystander UICs, and (iii) autophagy pre-induction in UICs would enhance IL-6

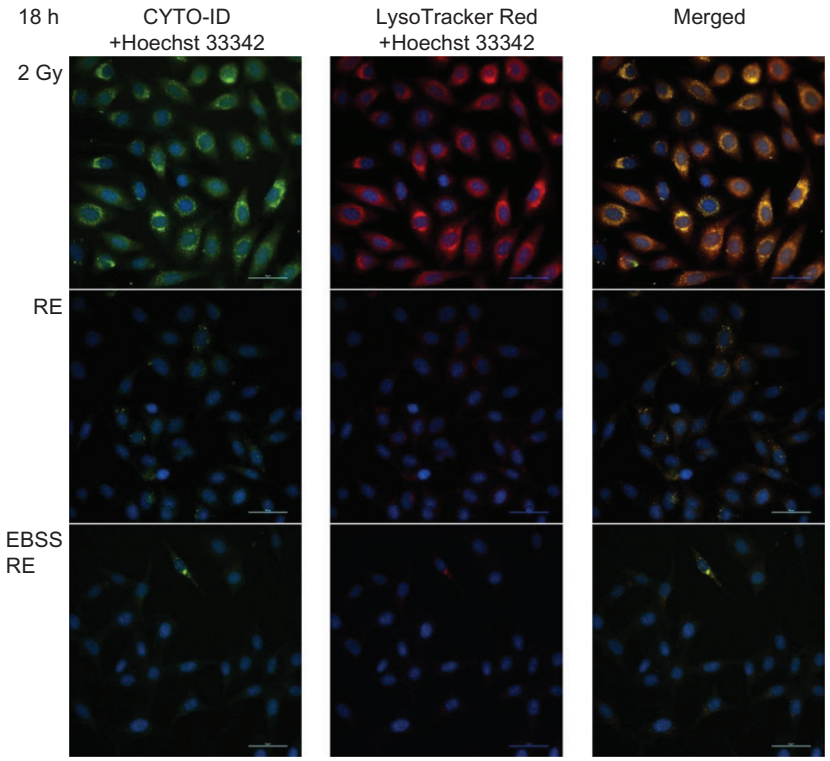

Fig. 8. Representative microscopic fields of HeLa cells with active autophagy (green) and AVOs (red) in different groups at 18 h post irradiation at ×40 magnification. Cell nuclei were counterstained with Hoechst 33342 (blue). Scale bar = 50 μm.

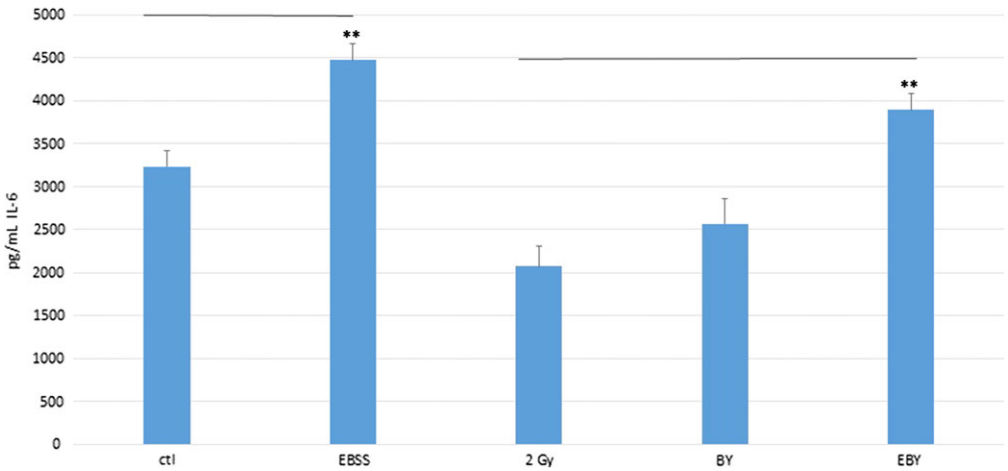

Fig. 9. IL-6 concentrations (pg/ml) measured using ELISA in different conditioned media from HeLa cells. Experiments were repeated three times independently. The data were analyzed using one-way ANOVA. *Post-hoc t*-tests were then performed to assess the statistical significance of difference between two particular groups. $^{**}P < 0.01$, and the bars represent ± SEM.

secretion in these UICs as well as RIRE in IRCs, RIRE was interpreted as a metabolic cooperation process. Some insights can be gained from this unified scheme:

(i) The stressed cells in the PCC/PSC system proliferated while deprived of nutrients, which actually is also the case for many cancer cells in a tumor microenvironment when the vascular supply of nutrients becomes limiting [15–19]; so in analogy, the NF-κB pathway was activated in the stressed cells in the IRC/UIC system (possibly promoting cell repair), while deprived of molecules to activate the NF-κB pathway. Knowledge about the process or the rescue

factor might help predict or improve the efficacy of the radiotherapy methods. In fact, NF-κB activation led to resistance of cancer cells to radio- and chemotherapies [64–67]. Accordingly, the sensitivity of a number of cancer cell lines to radiation treatment could be enhanced through inactivation of the NF-κB pathway in the IRCs [64–67]. Inactivation of autophagy pathways in UICs might also potentially lower the resistance of cancer cells to radiotherapies.

(ii) The bystander factors for the PCC/PSC system were not known. However, as inspired by the RIRE in the IRC/UIC system, the bystander factors are likely to be multiple, and may include TNF-α [68], TGF-β1 [69], IL-6 [70], IL-8 [71], NO [72–74] and ROS [75]. Once the bystander factors are identified, alternative therapy methods for pancreatic cancers and other cancers involving metabolic cooperation can be explored in terms of inhibiting the pathways in the cancer cells for secreting these bystander factors.

(iii) The unified scheme describing metabolic cooperation between stressed cells and bystander cells might help explain some unexpected results from previous studies on RIRE. When RIRE was first established, it referred to the phenomenon that IRCs derived benefits from feedback signals released from bystander UICs [1]. Interestingly, an exacerbated detrimental effect was recently found in IRCs upon partnering with UICs [7, 8], which seemed to have contradicted the 'rescue effect'. In their experiment, the IRCs were human bronchial epithelial (Beas-2B) cells, while the UICs were human macrophage (U937) cells derived from histiocytic lymphoma. As such, based on the cell types alone, the U937-cell/Beas-2B-cell system could resemble the PCC/PSC system, in which the U937 cells and Beas-2B cells could be regarded as stressed and bystander cells, respectively. On the other hand, when considered within the IRC/UIC system, the U937 cells and Beas-2B cells could be regarded as bystander and stressed cells, respectively. In the end, the cells destined to provide more support than the support they receive would show exacerbated effects compared with the expected effects from its initial sustained stress, as shown by the Beas-2B cells (IRCs) in this case. This conjecture also aligns with the observations from a number of previous studies. Widel *et al.* [2] confirmed the rescue effect in irradiated human melanoma (Me45) cells co-cultured with non-irradiated normal human dermal fibroblasts (NHDFs), but revealed that non-irradiated Me45 cells did not rescue co-cultured irradiated Me45 cells or co-cultured irradiated NHDF cells. Desai *et al.* revealed that for irradiated lung adenocarcinoma (A549) cells, bystander human lung normal fibroblast (WI38) cells provided a much stronger rescue effect than bystander A549 cells [4]. In fact, when RIRE was first established, RIRE was also studied in irradiated HeLa cancer cells partnered with unirradiated normal NHLF cells, and it was concluded that normal cells could also rescue irradiated cancer cells [1]. No complications arise in this case since the HeLa cancer cells were unequivocally the 'stressed' cells, based either on the cell types or on the categorization in the IRC/UIC system.

CONFLICT OF INTEREST

There are no conflicts of interest.

FUNDING

Funding for covering the cost of publishing this article in open access was provided by the State Key Laboratory in Marine Pollution, City University of Hong Kong.

REFERENCES

1. Chen S, Zhao Y, Han W et al. Rescue effects in radiobiology: unirradiated bystander cells assist irradiated cells through intercellular signal feedback. *Mutat Res* 2011;706:59–64.
2. Widel M, Przybyszewski WM, Cieslar-Pobuda A et al. Bystander normal human fibroblasts reduce damage response in radiation targeted cancer cells through intercellular ROS level modulation. *Mutat Res* 2012;731:117–24.
3. Pereira S, Malard V, Ravanat JL et al. Low doses of gamma-irradiation induce an early bystander effect in zebrafish cells which is sufficient to radioprotect cells. *PLoS One* 2014;9:e92974.
4. Desai S, Kobayashi A, Konishi T et al. Damaging and protective bystander cross-talk between human lung cancer and normal cells after proton microbeam irradiation. *Mutat Res* 2014;763–4:39–44.
5. Lam RKK, Han W, Yu KN. Unirradiated cells rescue cells exposed to ionizing radiation: activation of NF-κB pathway in irradiated cells. *Mutat Res* 2015;782:23–33.
6. He M, Dong C, Xie Y et al. Reciprocal bystander effect between α-irradiated macrophage and hepatocyte is mediated by cAMP through a membrane signaling pathway. *Mutat Res* 2014;763–4:1–9.
7. Fu J, Yuan D, Xiao L et al. The crosstalk between α-irradiated Beas-2B cells and its bystander U937 cells through MAPK and NF-κB signaling pathways. *Mutat Res* 2016;783:1–8.
8. Fu J, Wan, J, Wang X et al. Signaling factors and pathways of α-particle irradiation induced bilateral bystander responses between Beas-2B and U937 cells. *Mutat Res* 2016;789:1–8.
9. Liu Y, Kobayashi A, Fu Q et al. Rescue of targeted nonstem-like cells from bystander stem-like cells in human fibrosarcoma HT1080. *Radiat Res* 2015;184:334–40.
10. Kobayashi A, Tengku Ahmad TAF, Autsavapromporn N et al. Enhanced DNA double-strand break repair of microbeam targeted A549 lung carcinoma cells by adjacent WI38 normal lung fibroblast cells via bi-directional signaling. *Mutat Res* 2017;803–5:1–8.
11. Choi VWY, Ng CYP, Cheng SH. α-Particle irradiated zebrafish embryos rescued by bystander unirradiated zebrafish embryos. *Environ Sci Technol* 2012;46:226–31.
12. Kong EY, Choi VW, Cheng SH. Some properties of the signals involved in unirradiated zebrafish embryos rescuing α-particle irradiated zebrafish embryos. *Int J Radiat Biol* 2014;90:1133–42.

13. Lam RK, Fung YK, Han W. Rescue effects: irradiated cells helped by unirradiated bystander cells. *Int J Mol Sci* 2015;16: 2591–609.
14. Palm W Thompson CB. Nutrient acquisition strategies of mammalian cells. *Nature* 2017;546:234–42.
15. Nieman KM, Kenny HA, Penicka CV et al. Adipocytes promote ovarian cancer metastasis and provide energy for rapid tumor growth. *Nat Med* 2011;17:1498–503.
16. Tardito S, Oudin A, Ahmed SU et al. Glutamine synthetase activity fuels nucleotide biosynthesis and supports growth of glutamine-restricted glioblastoma. *Nat Cell Biol* 2015;17: 1556–68.
17. Zhang W, Trachootham D, Liu J et al. Stromal control of cystine metabolism promotes cancer cell survival in chronic lymphocytic leukaemia. *Nat Cell Biol* 2012;14:276–86.
18. Sousa CM, Biancur DE, Wang X et al. Pancreatic stellate cells support tumour metabolism through autophagic alanine secretion. *Nature* 2016;536:479–83.
19. Muranen T, Iwanicki MP, Curry NL et al. Starved epithelial cells uptake extracellular matrix for survival. *Nat Commun* 2017; 8:13989.
20. Mayers JR, Wu C, Clish CB et al. Elevation of circulating branched-chain amino acids is an early event in human pancreatic adenocarcinoma development. *Nat Med* 2014;20:1193–8.
21. Das SK, Eder S, Schauer S et al. Adipose triglyceride lipase contributes to cancer-associated cachexia. *Science* 2011;333:233–8.
22. Djavaheri-Mergny M, Amelotti M, Mathieu J et al. NF-kappaB activation represses tumor necrosis factor-alpha-induced autophagy. *J Biol Chem* 2006;281:30373–82.
23. Djavaheri-Mergny M, Codogno P. Autophagy joins the game to regulate NF-kappaB signaling pathways. *Cell Res* 2007;17: 576–7.
24. Trocoli A, Djavaheri-Mergny M. The complex interplay between autophagy and NF-κB signaling pathways in cancer cells. *Am J Cancer Res* 2011;1:629–49.
25. Xiao G. Autophagy and NF-kappaB: fight for fate. *Cytokine Growth Factor Rev* 2007;18:233–43.
26. Rubinsztein DC. The roles of intracellular protein-degradation pathways in neurodegeneration. *Nature* 2006;443:780–6.
27. Komatsu M, Ichimura Y. Selective autophagy regulates various cellular functions. *Genes Cells* 2010;15:923–33.
28. Knaevelsrud H, Simonsen A. Fighting disease by selective autophagy of aggregate prone proteins. *FEBS Lett* 2010;584: 2635–45.
29. Johansen T, Lamark T. Selective autophagy mediated by autophagic adapter proteins. *Autophagy* 2011;7:279–96.
30. Gozuacik D, Kimchi A. Autophagy as a cell death and tumor suppressor mechanism. *Oncogene* 2004;23:2891–906.
31. Levine B, Klionsky DJ. Development by self-digestion: molecular mechanisms and biological functions of autophagy. *Dev Cell* 2004;6:463–77.
32. Kroemer G, Marino G, Levine B. Autophagy and the integrated stress response. *Mol Cell* 2010;40:280–93.
33. Dewaele M, Maes H, Agostinis P. ROS mediated mechanisms of autophagy stimulation and their relevance in cancer therapy. *Autophagy* 2010;6:838–54.
34. Fleming A, Noda T, Yoshimori T et al. Chemical modulators of autophagy as biological probes and potential therapeutics. *Nat Chem Biol* 2011;7:9–17.
35. Amaravadi RK, Lippincott-Schwartz J, Yin XM et al. Principles and current strategies for targeting autophagy for cancer treatment. *Clin Cancer Res* 2011;17:654–66.
36. Mizushima N, Levine B, Cuervo AM et al. Autophagy fights disease through cellular self-digestion. *Nature* 2008;451:1069–75.
37. Hino M, Hamada N, Tajika Y et al. Heavy ion irradiation induces autophagy in irradiated C2C12 myoblasts and their bystander cells. *J Electron Microsc* 2010;59:495–501.
38. Wang X, Zhang J, Fu J et al. Role of ROS-mediated autophagy in radiation-induced bystander effect of hepatoma cells. *Int J Radiat Biol* 2015;91:452–8.
39. Hirano T, Ishihara K, Hibi M. Roles of STAT3 in mediating the cell growth, differentiation and survival signals relayed through the IL-6 family of cytokine receptors. *Oncogene* 2000;19: 2548–56.
40. Heinrich PC, Behrmann I, Muller-Newen G et al. Interleukin-6-type cytokine signalling through the gp130/Jak/STAT pathway. *Biochem J* 1998;334:297–314.
41. Yoon S, Woo SU, Kang JH et al. STAT3 transcriptional factor activated by reactive oxygen species induces IL6 in starvation-induced autophagy of cancer cells. *Autophagy* 2010;6:1125–38.
42. Yoon S, Woo SU, Kang JH et al. NF-kB and STAT3 cooperatively induce IL6 in starved cancer cells. *Oncogene* 2012;31: 3467–81.
43. Scherz-Shouval R, Shvets E, Fass E et al. Reactive oxygen species are essential for autophagy and specifically regulate the activity of Atg4. *EMBO J* 2007;26:1749–60.
44. Zhou J, Tan SH, Nicolas V et al. Activation of lysosomal function in the course of autophagy via mTORC1 suppression and autophagosome–lysosome fusion. *Cell Res* 2013;23:508–23.
45. Klionsky DJ, Cuervo AM, Seglen PO. Methods for monitoring autophagy from yeast to human. *Autophagy* 2007;3:181–90.
46. Mitroulis I, Kourtzelis I, Papadopoulos VP et al. *In vivo* induction of the autophagic machinery in human bone marrow cells during *Leishmania donovani* complex infection. *Parasitol Int* 2009;58:475–80.
47. Pierzyńska-Mach A, Janowski PA, Dobrucki JW. Evaluation of acridine orange, LysoTracker Red, and quinacrine as fluorescent probes for long-term tracking of acidic vesicles. *Cytometry A* 2014;85:729–37.
48. Guo S, Liang Y, Murphy SF et al. A rapid and high content assay that measures cyto-ID–stained autophagic compartments and estimates autophagy flux with potential clinical applications. *Autophagy* 2015;11:560–72.
49. Oeste CL, Seco E, Patton WF et al. Interactions between autophagic and endo-lysosomal markers in endothelial cells. *Histochem Cell Biol* 2013;139:659–70.
50. Chan LL, Shen D, Wilkinson AR et al. A novel image-based cytometry method for autophagy detection in living cells. *Autophagy* 2012;8:1371–82.
51. Schmeisser H, Fey SB, Horowitz J et al. Type I interferons induce autophagy in certain human cancer cell lines. *Autophagy* 2013;9:683–96.

52. Asaithamby A, Chen DJ. Cellular responses to DNA double-strand breaks after low-dose γ-irradiation. *Nucleic Acids Res* 2009;37:3912–23.
53. Schultz LB, Chehab NH, Malikzay A et al. p53 Binding protein 1 (53BP1) is an early participant in the cellular response to DNA double-strand breaks. *J Cell Biol* 2000;151:1381–90.
54. Hino M, Wada S, Tajika Y et al. Heavy ion microbeam irradiation induces ultrastructural changes in isolated single fibers of skeletal muscle. *Cell Struct Funct* 2007;32:51–6.
55. Hino M, Hamada N, Tajika Y et al. Insufficient membrane fusion in dysferlin-deficient muscle fibers after heavy-ion irradiation. *Cell Struct Funct* 2009;34:11–5.
56. Oishi T, Sasaki A, Hamada N et al. Proliferation and cell death of human glioblastoma cells after carbon-ion beam exposure: morphologic and morphometric analyses. *Neuropathology* 2008;28:408–16.
57. Jinno-Oue A, Shimizu N, Hamada N et al. Irradiation with carbon ion beams induces apoptosis, autophagy, and cellular senescence in a human glioma-derived cell line. *Int J Radiat Oncol Biol Phys* 2010;76:229–41.
58. Jin X, Li F, Zheng X et al. Carbon ions induce autophagy effectively through stimulating the unfolded protein response and subsequent inhibiting Akt phosphorylation in tumor cells. *Sci Rep* 2015;5:13815.
59. Paglin S, Hollister T, Delohery T et al. A novel response of cancer cells to radiation involves autophagy and formation of acidic vesicles. *Cancer Res* 2001;61:439–44.
60. Lomonaco SL, Finniss S, Xiang C et al. The induction of autophagy by γ-radiation contributes to the radioresistance of glioma stem cells. *Int J Cancer* 2009;125:717–22.
61. Huang YH, Yang PM, Chuah QY et al. Autophagy promotes radiation-induced senescence but inhibits bystander effects in human breast cancer cells. *Autophagy* 2014;10:1212–8.
62. Mutou-Yoshihara Y, Funayama T, Yokota Y et al. Involvement of bystander effect in suppression of the cytokine production induced by heavy-ion broad beam. *Int J Radiat Biol* 2012;88:258–66.
63. Tamari Y, Kashino G, Mori H. Acquisition of radioresistance by IL-6 treatment is caused by suppression of oxidative stress derived from mitochondria after γ-irradiation. *J Radiat Res* 2017;58:412–20.
64. Mayo MW, Baldwin AS. The transcription factor NF-B: control of oncogenesis and cancer therapy resistance. *Biochim Biophys Acta* 2000;1470:M55–62.
65. Bharti AC, Aggarwal BB. Nuclear factor-kappa B and cancer: its role in prevention and therapy. *Biochem Pharmacol* 2002;64:883–8.
66. Luo JL, Kamata H, Karin M. IKK/NF-κB signaling: balancing life and death—a new approach to cancer therapy. *J Clin Invest* 2005;115:2625–32.
67. Nakanishi C, Toi M. Nuclear factor-kappaB inhibitors as sensitizers to anticancer drugs. *Nat Rev Cancer* 2005;5:297–309.
68. Shareef MM, Cui N, Burikhanov R et al. Role of tumor necrosis factor-alpha and TRAIL in high-dose radiation-induced bystander signaling in lung adenocarcinoma. *Cancer* 2007;67:11811–20.
69. Iyer R, Lehnert BE, Svensson R. Factors underlying the cell growth–related bystander responses to alpha particles. *Cancer Res* 2000;60:1290–8.
70. Chou C-H, Chen P-J, Lee P-H et al. Radiation-induced hepatitis B virus reactivation in liver mediated by the bystander effect from irradiated endothelial cells. *Clin Cancer Res* 2007;13:851–7.
71. Facoetti A, Ballarini F, Cherubini R et al. Gamma-ray-induced bystander effect in tumour glioblastoma cells: a specific study on cell survival, cytokine release and cytokine receptors. *Radiat Prot Dosimetry* 2006;122:271–4.
72. Matsumoto H, Hayashi S, Hatashita M et al. Induction of radioresistance by a nitric oxide–mediated bystander effect. *Radiat Res* 2001;155:387–96.
73. Han W, Wu L, Chen S et al. Constitutive nitric oxide acting as a possible intercellular signaling molecule in the initiation of radiation-induced DNA double strand breaks in non-irradiated bystander cells. *Oncogene* 2007;26:2330–9.
74. Shao C, Folkard M, Prise KM. Role of TGF-β1 and nitric oxide in the bystander response of irradiated glioma cells. *Oncogene* 2008;27:434–40.
75. Shao C, Furusawa Y, Kobayashi Y et al. Bystander effect induced by counted high-LET particles in confluent human fibroblasts: a mechanistic study. *FASEB J* 2003;17:1422–7.